

ON NONEQUILIBRIUM RADIATION IN HYDROGEN SHOCK LAYERS

Chul Park

Department of Aerospace Engineering, Korea Advanced Institute of Science and Technology, Guseong-dong, Yuseong-gu, Daejeon, 305-701 Korea, cpark216@kaist.ac.kr

ABSTRACT

The influence of thermochemical nonequilibrium in the shock layer over a vehicle entering the atmosphere of an outer planet is examined qualitatively. The state of understanding of the heating environment for the Galileo Probe vehicle is first reviewed. Next, the possible reasons for the high recession in the frustum region and the low recession in the stagnation region are examined. The state of understanding of the nonequilibrium in the hydrogen flow is then examined. For the entry flight in Neptune, the possible influence of nonequilibrium is predicted.

1. INTRODUCTION

Entry flight into Jupiter has been accomplished in Project Galileo. In the future, exploration into other outer planets such as Saturn, Uranus, or Neptune is possible. The atmospheres of these outer planets consist of a mixture of hydrogen and helium. In the shock layer over the entry vehicle, hydrogen tends to be ionized. Ionization of hydrogen produces radiation which, depending on the condition, may be strong. In order to design the heatshields for these outer planet probe vehicles efficiently, one needs to examine how the heatshield for the Galileo Probe vehicle performed.

In the case of Galileo Probe, heating was expected to be mostly by radiation. Prior to the Galileo Probe mission, theoretical prediction of the surface recession of the heatshield for the Probe vehicle has been made by, among others, Moss and Simmonds [1]. The surface recession of the Galileo Probe heatshield in the flight data was found to be substantially different from the predictions, as shown in Fig. 1.

In the figure, the abscissa is the ratio of the radial chord length along the surface s to the nose radius R . As seen in the figure, the recession in the flight was greater than the prediction by Moss and Simmonds by a ratio of 1.74 to 1 in the frustum and smaller than the prediction by a ratio of 0.77 to 1 at the stagnation point.

Shown also in Fig.1 is the latest calculation by Matsuyama et al [2]. Their calculation reproduced the recession values in the frustum region closely. The

difference between their calculation and the calculation by Moss and Simmonds [1] is in the assumed intensity of turbulence; turbulence is more intense in the latest calculation in the region adjacent to the ablating wall. In the calculation by Moss and Simmonds, turbulence intensity was assumed to be zero at wall, following the existing turbulence model for flows over a smooth wall. In the calculation by Matsuyama et al, it is assumed to be finite at wall. There are several possible reasons why turbulence intensity could be finite at wall. Among these possible reasons, Matsuyama et al have chosen the injection-induced turbulence model of Park [3] to explain it.

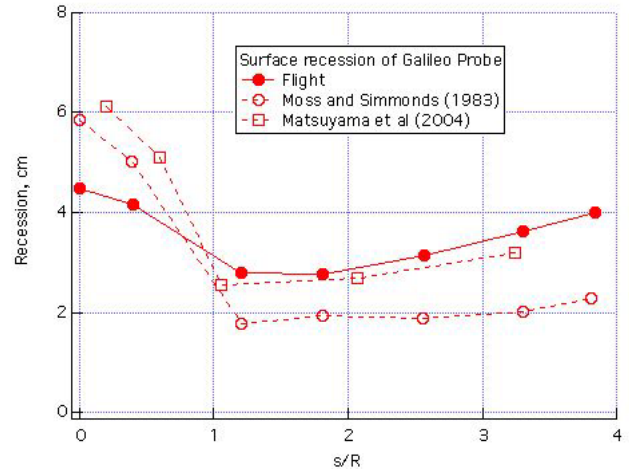


Fig. 1. Comparison of the predicted and measured recessions of the Galileo Probe heatshield.

According to the injection-induced turbulence model, the ablation product gas is inherently turbulent when it emerges from the surface of an ablating heatshield. The finite turbulence intensity at wall disperses the ablation product species, C_3 , faster into the flow, and thus reduces its concentration in the region near the wall, as shown in Fig. 2. This leads to smaller radiation absorption by C_3 , and hence larger radiative heat flux reaching the wall.

It is to be noted here that Matsuyama et al did not account for the increase in convective heating rate due to surface roughness. If it is accounted for, the

calculated heating rate in the frustum region will become even larger.

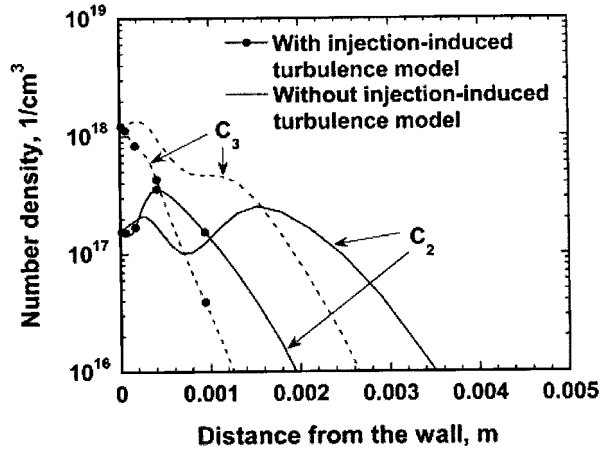


Fig. 2. Distribution of C_3 and C_2 in the boundary layer at the location of ARAD 7-8 in the frustum region calculated by Matsuyama et al [2].

The agreement between the theory and calculation in the frustum region leaves only the stagnation region behavior in the recession data to be explained. There are three possible explanations as to why the recession in the stagnation region is over-predicted. They are:

a) *Spallation*: Carbonaceous heatshield materials produce solid particles at their surface and inject them into the shock layer flow with a finite speed [4-6]. This phenomenon is referred to commonly as spallation. These solid particles travel to the inviscid region of the shock layer. There, the particles vaporize and the resulting carbon atoms partially ionize. The process of vaporization and ionization absorb energy, and thereby cool the flow and reduce radiation emission.

c) *Radiation Absorption*: The ablation product gas contains species that are not accounted for in the calculation but absorb radiation. The phenolic resin in the heatshield contains a substantial concentration of hydrogen and a small concentration of oxygen. These will form CH and CO. CO will absorb in the wavelength region shorter than 2000 Å. CH will absorb from about 3500 to about 5000 Å. CO is long-lived because of its strong bonding. But CH will decompose rapidly because of its weak bonding. Exactly how much of these two species exist in the boundary layer and how much radiation they will absorb are unknown at this time.

c) *Nonequilibrium*: The region immediately downstream of the bow shock wave is undergoing dissociation and ionization. A finite time is required for

the ionization equilibrium is reached. In the nonequilibrium region prior to reaching equilibrium, electron density will be low or nonexistent. This nonequilibrium region will emit radiation smaller than the equilibrium region or none at all. Radiative heat flux reaching the ablating wall will be reduced correspondingly. This possibility was first proposed by Howe [7].

None of these three possible explanations has been explored in detail. It is the purpose of the present work to explore the nonequilibrium explanation, c).

2. EQUILIBRATION TIME

Howe based his arguments on the shock tube experiment conducted by Leibowitz [8]. Leibowitz studied the evolution of electron density behind a shock wave in a 21% H_2 -79% He mixture. The shock tube was driven by an electric arc-heated driver gas shown schematically in Fig. 3. The driver section was in the shape of a cone. In the experiment, the intensity of the radiation emitted behind the moving shock wave at 5145 Å, which is known to be proportional to the square of electron density, was measured as a function of time as shown in Fig. 4. The ionization equilibration time, or relaxation time for ionization, t_{lab} , was defined from the oscillogram trace as shown. The true relaxation time, ∞ is t_{lab} multiplied by the density ratio across the shock wave, which was typically 5 in the experiment.

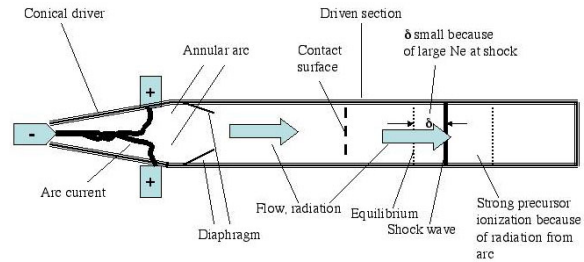


Fig. 3. Schematic of a conical electrically-driven shock tube used by Leibowitz [8] and Bogdanoff and Park [11].

The true relaxation time ∞ determined in Leibowitz's experiment, multiplied by the number density of H_2 molecules behind the shock wave, is shown as a function of the reciprocal of the post-shock translational temperature prior to vibrational excitation or chemical reaction (dissociation and ionization) T_s in Fig. 5.

Subsequently, Livingston and Poon [9] repeated the experiment in a shock tube driven by an electric arc configured in an annular geometry, as shown

schematically in Fig. 6. Their data are compared with Leibowitz's data in Fig. 5.

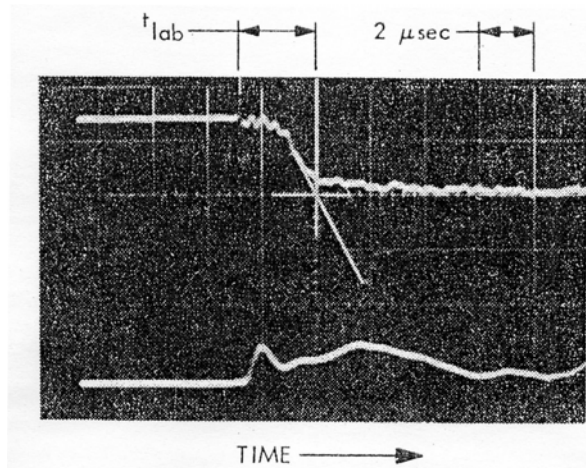


Fig. 4. Oscilloscope trace of continuum radiation at 5145 A in the shock experiment of Leibowitz [7] showing the definition of the ionization equilibration (relaxation) time in the laboratory frame t_{lab} .

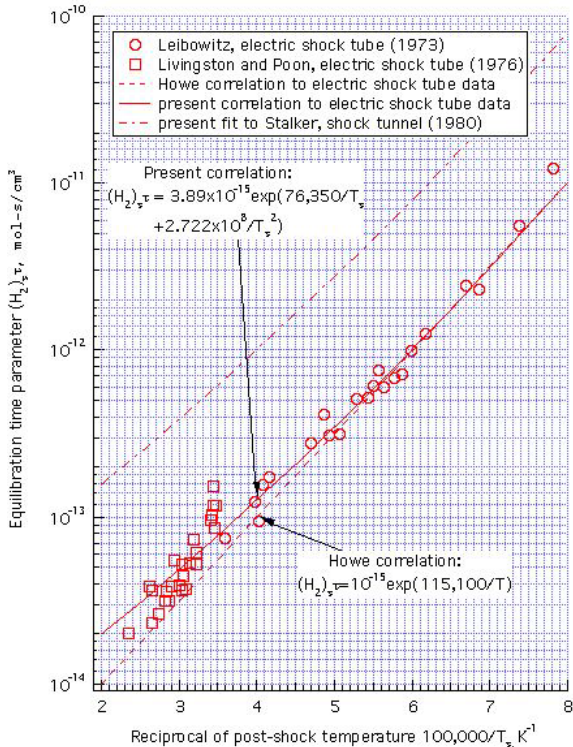


Fig. 5. The product of the number density of H₂ behind shock and the equilibration time t plotted as a function of $1/T_2$.

Still later, Stalker [10] measured the relaxation time in a shock tunnel experiment. In that experiment, the test

flow was produced in the test section of a shock tunnel. An inclined flat plate was placed in the test flow, and density variation behind the oblique shock wave was determined by an interferometer, as shown schematically in Fig. 7. The equilibration distance so obtained is shown by a dash curve in Fig. 5.

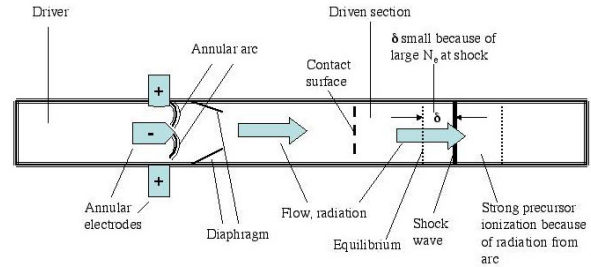


Fig. 6. Schematic of the annular-arc driven shock tube used by Livingston and Poon [9].

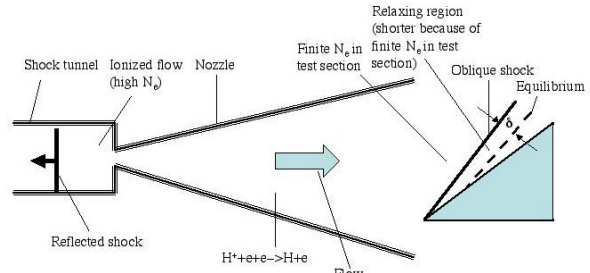


Fig. 7. Schematic of the shock tunnel experiment of Stalker [9].

As seen in Fig. 5, the data by Leibowitz and that by Livingston and Poon lie roughly on a straight line. Howe fitted Leibowitz's data by a straight line in this semi-log plot producing the correlation formula shown in the figure. A slightly more accurate correlation is derived here as

$$(H_2)_s \infty = 3.89 \times 10^{-15} \exp(76,350/T_s) + 2.722 \times 10^8 / T_s^2 \quad \text{mol-sec/cm}^3 \quad (1)$$

The relaxation time values obtained by Stalker [10] is 7.9 times longer than the values given by this expression, as shown in Fig. 5.

The substantial disagreement between the two sets of data on relaxation time casts doubt on both sets. A clue to the inadequacy of the two sets of data obtained by an arc-driven shock tube is in the measured values of electron density in the experiment by Livingston and Poon shown in Fig. 8. In the figure, the solid curve is the theoretical equilibrium value determined from the Rankine-Hugoniot relations assuming no radiative cooling. The dash curve shows the equilibrium values accounting for radiative cooling by the emission of Balmer lines in the wavelength range from 4300 to

6600 A that occur during the travel of 3 meters. As seen in the figure, measured electron density is substantially larger than the theoretical values.

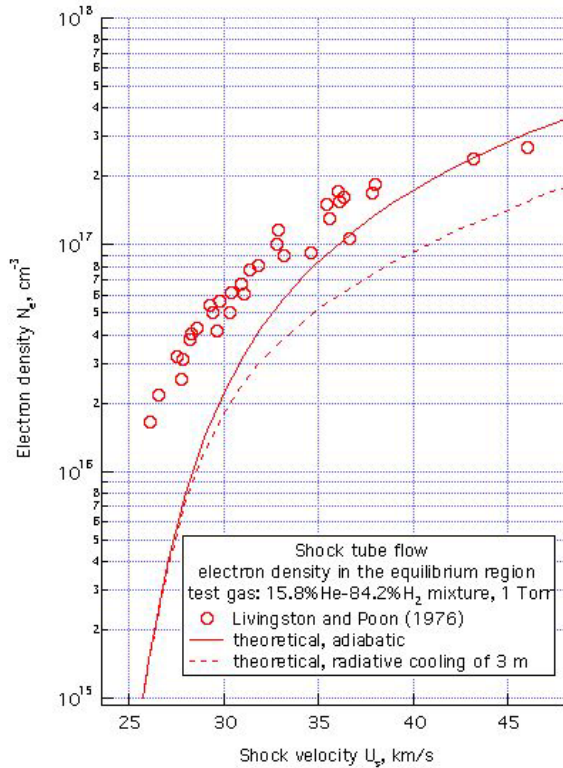


Fig. 8. Comparison between the measured and calculated electron density in the equilibrium region behind the shock wave in the experiment by Livingston and Poon [9].

Bogdanoff and Park [11] attempted to recreate the works of Leibowitz and Livingston and Poon in a shock tube of a design very similar to that used by Leibowitz. They found that the measured electron densities are much larger than the theoretical equilibrium values. They investigated the cause of this discrepancy, and found that the radiation emitted in the arc in the driver ionized the test gas flow behind the shock wave. Thus, the data by Leibowitz and Livingston and Poon are rendered inaccurate.

The data by Stalker is not totally trustworthy either. In his experiment, the flow in the reflected region is highly ionized. In the expanding nozzle, electron recombination occurs. But the recombination is not expected to be completed: finite concentration of electrons is bound to exist in the test section. The rate of the ionization process



Depends very strongly on the concentration of electrons in front of the shock wave. Presence of electrons in the test section will tend to shorten the relaxation time behind the shock wave.

Thus, none of the existing data on the ionization relaxation time can be trusted. The true value of ∞ should be longer than the Stalker value shown in Fig. 5. A new experiment is being carried out at NASA Ames Research Center which is free from the impediments encountered in those past experiments is presently being carried out. One must wait for the outcome of the experiment to correctly assess the nonequilibrium problem.

3. NONEQUILIBRIUM PROCESSES

The nonequilibrium processes occurring in the shock layer are shown schematically in Fig. 9. These processes are described in one-dimensional flow in Fig. 10.

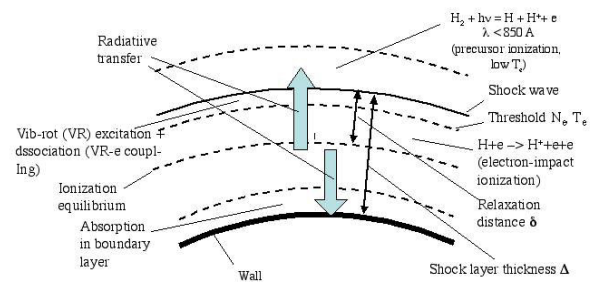


Fig. 9. Schematic of the nonequilibrium processes in shock layer.

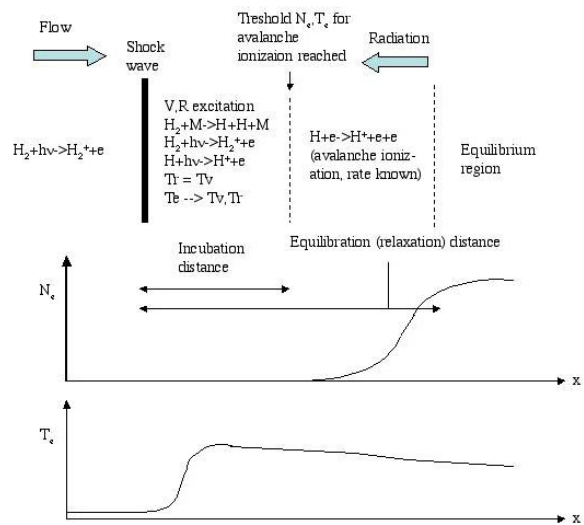
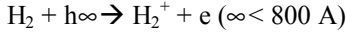
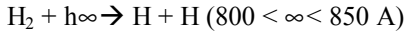


Fig.10. Schematic of nonequilibrium process behind a normal shock wave.

As shown in these figures, in front of the bow shock wave, H₂ starts to be dissociated and ionized by



The second process, photo-ionization, leads to the so-called precursor ionization. The cross section for these two processes have been measured by Cook and Metzger [12], and are shown in Fig. 11. According to the data, the strongest absorption occurs at 700 Å with a cross section of about 10⁻¹⁷ cm².

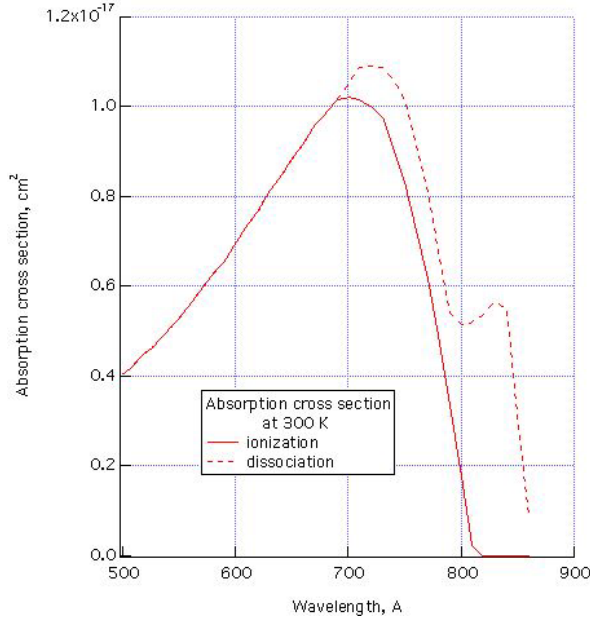


Fig. 11. Absorption cross section of H₂ for photo-dissociation and photo-ionization, from Cook and Metzger [12].

The radiation emitted by the ionized flow behind the shock wave propagates upstream as shown in Figs. 9 and 10. In the freestream flow in front of the shock wave, the radiation is absorbed by the cross section shown in Fig. 11. The radiation intensity decays there exponentially with distance according to the Beer's law. The e-folding distance of the radiation is given by

$$\text{e-folding distance} = 1/(\infty n)$$

where ∞ is the cross section and n is the number density of H₂. The e-folding distance is shown for the Galileo Probe entry in Fig. 12. As shown, the e-folding distance is nearly 1 cm at the peak heating point. In the experiment by Bogdanoff and Park [11], the precursor ionization was detected to a distance of several centimeters. Electrons produced by the precursor ionization process is at a low temperature, but its exact value is unknown.

Behind the shock wave, vibrational and rotational excitation and dissociation of H₂ occur. According to Furudate et al [13], vibrational and rotational temperatures are locked together here. Electron temperature will tend to couple with the vib-rotational mode here. However, the exact extent of the coupling is unknown at this time. As vib-rotational temperature rises, electron temperature will rise also. At a certain point, the threshold value of electron density will be reached to trigger the avalanche ionization process.

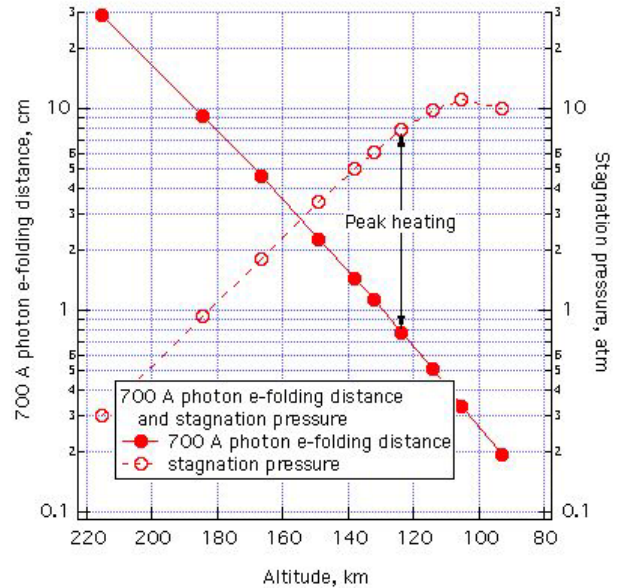


Fig. 12. The e-folding distance for decay of 700 Å radiation in front of the shock wave.

The distance from the shock wave to the threshold point is the incubation distance. It is this distance which is unknown at this time. All three existing sets of experiment [8-10] suffered from uncertainties as described above. Currently, theoretical work is being carried out on this topic by Furudate and Chang [15]. Once the avalanche ionization is started, the process can be predicted relatively accurately, because the ionization process of H is well known from both theory and experiment. It is to be noted here that the rate of the avalanche ionization will be influenced by the radiative transfer phenomenon, as described by Park [14].

In the incubation region, density of the flow will not change rapidly. Density will change rapidly as the avalanche ionization occurs. The interferogram of Stalker [10] shows this trend. The difference between the two sets of data obtained by an arc-driven shock tube [8,9] and the shock tunnel data [10] is the difference in the length of the incubation distance.

4. INFLUENCE ON RADIATIVE FLUX

For the Galileo Probe at its peak heating point, the distance to the ionization equilibrium point ∞ is calculated using the relaxation time values of Stalker [10], and are shown as a function of the normalized chord length s/R in Fig. 13. The thickness of the radiating layer, i.e. the layer with equilibrium ionization, is shown as a ratio to the shock layer thickness. As seen here, the thickness of radiating layer is substantially smaller than the shock layer thickness.

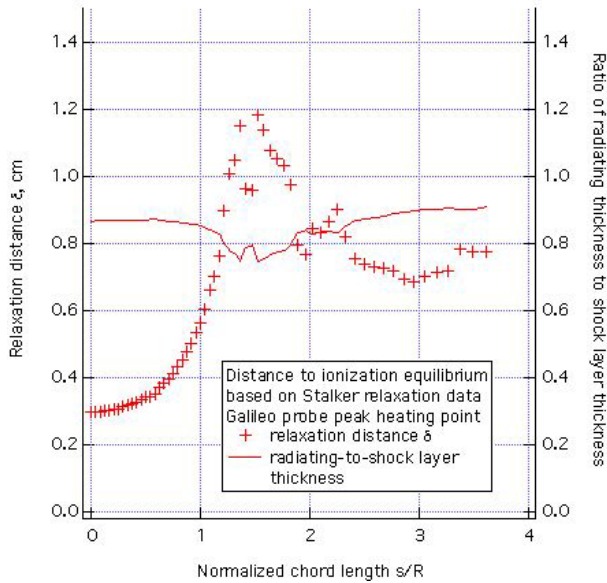


Fig. 13. Relaxation distance behind the bow shock for Galileo at its peak heating point calculated by Stalker's [10] relaxation data and the resulting radiating thickness expressed by its ratio to the shock layer thickness.

In Fig. 14, the electron density distribution across the shock layer is shown at two points, the stagnation point and a frustum point $s/R = 2$, resulting from the ionization nonequilibrium phenomenon. Two sets of relaxation distance were used here: the Stalker value and 2.5 times the Stalker value. For both cases, the electron density distribution becomes truncated because of the nonequilibrium phenomenon. For the stagnation point, the total number density of electrons has been significantly reduced by the truncation, especially for the 2.5 times Stalker value case. One can imagine that the radiative flux reaching the ablating wall will be reduced accordingly, because intensity of radiation emitted by a unit volume is approximately proportional to the square of electron density. However, for the frustum point, the truncation occurs in the region of low electron density. Therefore, one expects little decrease in radiative flux reaching the wall at the frustum point.

In Fig. 15, the estimated surface recessions for the Galileo Probe at the two points are shown. These estimated values are obtained by multiplying the recession values of Matsuyama et al in Fig. 1 by the ratio of the emitting thickness to the shock layer thickness at the peak heating point. The exact value can be known, of course, through a detailed calculation.

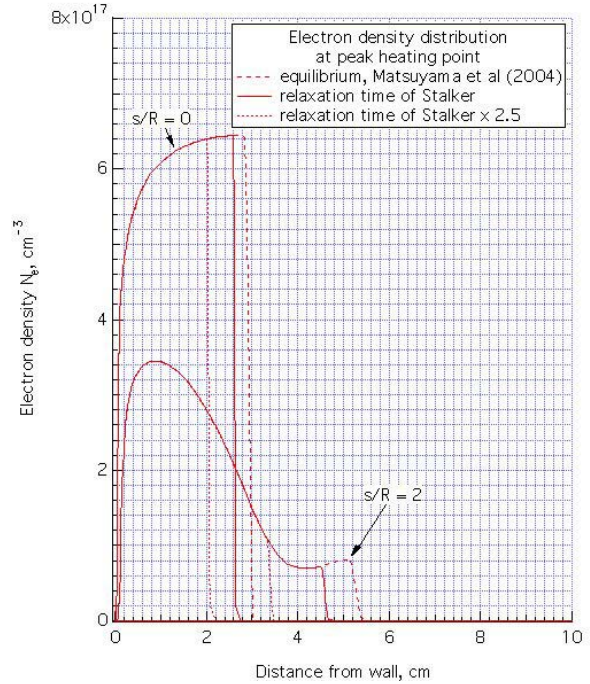


Fig. 14. Electron density profile across the shock layer at stagnation point and a frustum point accounting for the nonequilibrium phenomenon.

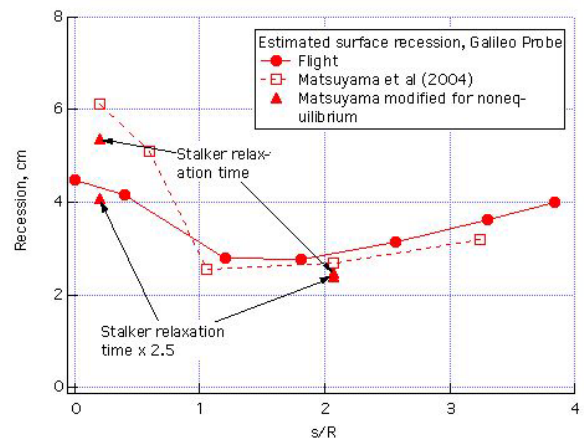


Fig. 15. Estimated surface recessions accounting for nonequilibrium, determined by Stalker's relaxation time and 2.5 times Stalker's relaxation times.

As seen in Fig. 15, if the relaxation time is 2.5 times Stalker's value, then the calculated recession should approximately agree with the flight data.

In Fig. 16, the ionization equilibration distance behind the normal shock wave is calculated for a typical aerobraking flight through the atmosphere of Neptune. The atmosphere is considered to consist of 20%He-80%H₂ mixture. The relaxation time data of Stalker [10] is used here.

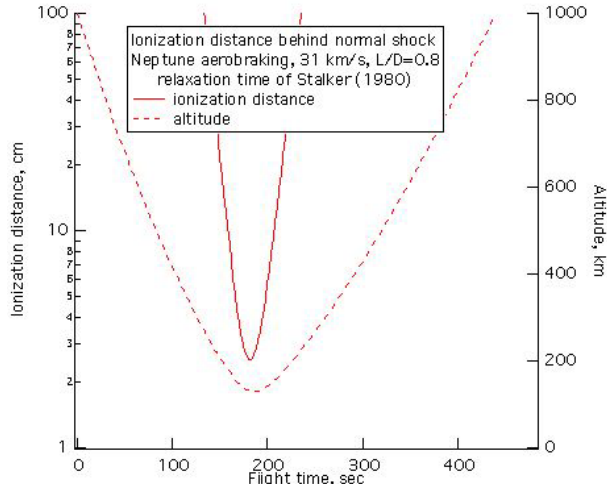


Fig. 16. Ionization relaxation distance behind a normal shock wave during the aerobraking flight through Neptune calculated using the relaxation time data of Stalker [10]; ballistic coefficient = 400 kg/m², L/D = 0.8, entry velocity at 1000 km altitude = 31.3 km/s.

As seen in the figure, the relaxation distance is about 2.5 cm at the perigee. This means that the nonequilibrium phenomenon will be very significant in the Neptune entry flight.

5. DISCUSSION

As seen in Fig. 15, the nonequilibrium phenomenon will successfully explain the low recession of Galileo Probe heatshield in the stagnation region without raising the recession in the frustum region, if the true relaxation time is longer than that given by Stalker [10]. It is highly desirable that the true relaxation time be determined experimentally. Theoretical works, such as that by Furudate and Chang [15] is desirable also.

As mentioned in Introduction, ionization nonequilibrium is one of the three possible causes of the observed low recession of the Galileo Probe heatshield in the stagnation region. The other two possible explanations should be pursued also.

6. CONCLUSIONS

The existing experimental data on ionization equilibration time taken in arc-driven shock tubes greatly underestimate because of the radiation from the driver. The experimental data obtained in a shock tunnel, which is 8 times that taken in arc-driven shock tubes, is likely to be underestimating still because of the nonequilibrium in nozzle flow. If the true equilibration time is 2.5 times that determined in a shock tunnel, the low surface recession at the stagnation point of Galileo Probe is explained. For Neptune entry, nonequilibrium effect will be even more significant. Uncertainty regarding the equilibration time concerns the processes prior to reaching the threshold of avalanche ionization.

7. REFERENCES

1. Moss, J. N., and Simmonds, A. L., "Galileo Probe Forebody Flowfield Predictions," *Entry Vehicle Heating and Thermal Protection Systems: Space Shuttle, Solar Starprobe, Jupiter Galileo Probe*, Progress in Astronautics and Aeronautics, Vol. 85, edited by P. E. Bauer and H. E. Collicott, AIAA New York, 1983, pp. 419-445.
2. Matsuyama, S., Ohnishi, N., Sasoh, A., and Sawada, K., "Numerical Simulation of Galileo Probe Entry Flowfield with Radiation and Ablation," AIAA Paper 2002-2994; to be published in *Journal of Thermophysics and Heat Transfer*.
3. Park, C., "Injection-Induced Turbulence in Stagnation Point Boundary Layers," *AIAA Journal*, Vol. 22, No. 2, February 1984, pp. 219-225.
4. Lundell, J. H., and Dickey, R. R., "Response of Heat-Shield materials to Intense Laser Radiation," AIAA Paper 78-0138, January 1978.
5. Davies, C. B., and Park, C., "Trajectories of Solid Particles Spalled from a Carbonaceous Heat Shield," *Entry Vehicle Heating and Thermal Protection Systems: Space Shuttle, Solar Starprobe, Jupiter Galileo Probe*, Progress in Astronautics and Aeronautics, Vol. 85, edited by P. E. Bauer and H. E. Collicott, AIAA, 1983, pp. 472-495.
6. Park, C., Raiche, G. A., and Driver, D. M., "Radiation of Spalled Particles in Shock Layers," to be published in *Journal of Thermophysics and Heat Transfer*.
7. Howe, J. T., "Hydrogen Ionization in the Shock Layer for Entry into the Outer Planets," *AIAA Journal*, Vol. 12, No. 6, June 1974, pp. 875-876.
8. Leibowitz, L. P., "Measurements of the Structure of an Ionizing Shock Wave in a Hydrogen-Helium Mixture," *The Physics of Fluids*, Vol. 16, No. 1, January 1973, pp. 59-68.

9. Livingston, F. R., and Poon, P. T. Y., "Relaxation Distance and Equilibrium Electron Density Measurements in Hydrogen-Helium Plasmas," AIAA Journal, Vol. 14, No. 9, September 1976, pp. 1335-1337.
10. Stalker, R. J., "Shock Tunnel Measurement of Ionization Rates in Hydrogen," AIAA Journal, Vol. 18, No. 4, April 1980, pp. 478-480.
11. Bogdanoff, D. A., and Park, C., "Radiative Interaction Between Driver and Driven Gases in an Arc-Driven Shock Tube," Shock Wave, Vol. 12, No. 3, November 2002, pp. 205-214.
12. Cook, and Metzger, Journal of Optical Society of America, Vol. 54, No. 8, August 1964, pp. 968-972.
13. Furudate, M., Fujita, K., and Abe, T., "Coupled Rotational-Vibrational Relaxation of Molecular Hydrogen at High Temperatures," AIAA Paper 2003-3780, 2003.
14. Park, C., "Effect of Lyman Radiation on Nonequilibrium Ionization of Atomic Hydrogen," AIAA Paper 2004-2277, 2004.
15. Furudate, M., and Chang, K. S., "Calculation of H₂-He Flow with Nonequilibrium Ionization and Radiation: Interim Report," paper presented at the 2nd Planetary Probe Workshop.